Numerical models for biocompatible shape memory materials and their biomedical applications

Melnik, R.V.N., Wang, L. and Mahapatra, D.R.

In: Proceedings of the 17th IMACS World Congress on Scientific Computation, Applied Mathematics and Simulation, Eds. Borne P. et al, ISBN 2-915913-02-1, 7 pages, 2005.

Numerical Models for Biocompatible Shape Memory Materials and Their Biomedical Applications

R.V.N. Melnik[1], **L. Wang**[2], **and D. R. Mahapatra**[1]

[1]Mathematical Modelling & Computational Sciences,
Wilfrid Laurier University, 75 University Ave W.,
Waterloo, ON, Canada N2L 3C5
Phone: +1-519884-1970(3662), Fax: +1-519-884-9738, E-mail: rmelnik@wlu.ca

[2]Mads Clausen Institute, Syddansk University,
Grundtvigs Alle 150, Sonderborg, DK-6400, Denmark

Abstract - Properties of shape memory alloys are becoming increasingly important in biomedical applications. In this paper, we analyse numerically a model for the description of the dynamic of such materials, focusing on a specific type of phase transformations. Starting from a general nonlinear system of conservation laws, we show how it can be reduced to the 2D case and how the resulting model can be discretized. Several numerical examples are presented.

Keywords—**Shape memory alloy patches; biomedical applications; differential-algebraic systems; systems biology.**

I. INTRODUCTION

Biomaterials have a thousand year history and photopolymerization, used by the ancient Egyptians for mummification, as well as applications of gold in dentistry are just a few of many examples [LAN 04]. Today, new biomaterials are designed with the idea to integrate them in a best possible way with systems biology and preserve properties present in biological systems. One such property that has an increasing importance in biology and medicine is shape memory. This property is critical in orthodentistry, distraction osteogenesis, suture tendon and many other applications. The materials of choice in such cases are often shape memory alloys (SMA) which have excellent biocompatibility properties (e.g., [KUJ 04]).

The Shape Memory Effect (SME) in SMA implies that upon the action of thermal, magnetic, electrical, hydrostatic and other fields, the SMAs can recover their original shape after being permanently deformed. This effect has been a subject of considerable theoretical and experimental efforts (e.g. [BIR 97] and references therein). The current situation is such that engineering and biomedical applications of SMA out paced the development of adequate mathematical and physical theories for modelling these materials. Such theories are needed in order to bridge the gap between engineering and biomedical applications of SMA and our ability to predict/model the response of the material under various loadings.

However, even for the one dimensional cases, the analysis of the dynamics of the SMAs structures is quite involved due to martensitic phase transformations, the strong nonlinearity in the mechanical field, and a strongly nonlinear pattern of interaction between mechanical and thermal fields ([MEL 01], [BIR 97], [MEL 02], [BUB 96], [FAL 90] and references therein). There are several important results on the development of free energy functionals in three dimensional cases on the basis of modified Landau-Ginzburg theory, but their numerical implementation is still not practical [FAL 90], [PAW 00], [ERI 86]. Recently, for the simulation of 2D microstructures in ferro-elastic materials, several models were proposed [ICH 00], [JAC 00]. The models were derived from the 3D model, but no thermomechanical coupling was discussed and only static simulations of microstructures on a mesoscale with fixed temperature were presented.

In this contribution, we analyse numerically a model for the description of the behaviour of SMA materials. In particular, we start our discussion from a general nonlinear system of conservation laws exemplified for a specific type of phase transformations [MAT 04]. We show how this model can be discretized by reducing it to a system of differential-algebraic equations. Finally, we present several numerical examples that demonstrate the application of the proposed technique to modelling the dynamics of SMA materials.

II. MATHEMATICAL MODEL

The model describing the dynamic behavior of SMAs patches is based on physical conservation laws and in the two-dimensional case can be written as follows [MEL 00]

$$\begin{aligned} \rho\frac{\partial^2 u_i}{\partial t^2} &= \nabla_x\cdot\vec{\sigma}+f_i, \quad i,j=1,2,\\ \rho\frac{\partial e}{\partial t}-\vec{\sigma}^T:(\nabla\mathbf{v})+\nabla\cdot\mathbf{q} &= g, \end{aligned} \tag{1}$$

where ρ is the density of the material, $\mathbf{u}=\{u_i\}|_{i=1,2}$ is the displacement vector, $\mathbf{v}=\partial\mathbf{u}/\partial t$ is the velocity vector, $\vec{\sigma}=\{\sigma_{ij}\}$ is the stress tensor, $\mathbf{q}$ is the heat flux, e is the internal energy, $\mathbf{f}=(f_1,f_2)^T$ and g are mechanical and thermal loadings, respectively.

In what follows, we consider a model for a specific type of transformations known as square-to-rectangular. Although idealized, such transformations can be regarded as a 2D analog of the cubic-to-tetragonal and tetragonal-to-orthorhombic transformations observed in general three-dimensional cases in a number of SMA materials (e.g., [JAC 00], [LOO 03] and reference therein). To start with, assume that the square lattice represents the austenite, while two rectangles represent the martensite variants. While this is an idealization in the 2D case, its 3D analogue leads us cubic-to-tetragonal and tetragonal-to-orthorhombic transformations observed in materials like Nb_3Sn, $InTl$, $FePd$ as well as in some copper based SMAs ([JAC 00], [SAX 98], [LOO 03] and reference therein).

Most numerical studies of the dynamics of phase transitions concerned mainly with the formation and growth of the related microstructures. They helped explain various phenomena, in particular on the mesoscale level, including the tweed microstructures ([KAR 95], [SAX 98], [JAC 00], [ICH 00], [LOO 03] and references therein).

According to Landau's theory, the basis of any nonlinear continuum-thermodynamics model for phase transitions is a non-convex free energy functional [ERI 86], [BAL 88], [LOO 03]. The global and local minima of the free energy potential with respect to the strain tensor (or deformation gradients) correspond to the stable and metastable states at a given temperature. A standard formalization of this leads to the Helmholtz free energy Ψ taken in the following form ([FAL 80], [FAL 90], [MEL 01], [MAT 04], [BUB 96] and references therein):

$$\Psi(\theta, \epsilon) = \psi_0(\theta) + \psi_1(\theta)\psi_2(\epsilon) + \psi_3(\epsilon) \tag{2}$$

where $\psi_0(\theta)$ models thermal field contribution, $\psi_1(\theta)\psi_2(\epsilon)$ models shape memory contributions and $\psi_3(\epsilon)$ models mechanical field contribution. The last two contributions can be simulated by one free elastic energy function which is dependent on the temperature. In the 1D case, $\epsilon = \partial u/\partial x$ is the strain, and it is chosen as the only order parameter for the phase transformations. The functions ψ_0 could be taken the following form

$$\psi_0 = -c_v\theta \ln \theta, \tag{3}$$

where c_v is the specific heat constant, θ_0 is the reference temperature for the transformation.

To characterize the austenite at high temperature and the martensite variants at low temperature in SMAs, a free elastic energy functional F was established earlier for the square to rectangular transformations, in which the classical Landau free energy function F_l [ICH 00], [JAC 00] was modified. For the square to rectangular transformation, only one order parameter is needed to characterize the martensite variants [FAL 90], [FAL 90], [LOO 03]. According to a number of authors ([LOO 03], [ICH 00], [JAC 00], [SAX 98], [KAR 95] and references therein), a simple free elastic energy functional could be chosen as a function of the order parameter as follows:

$$\begin{aligned} F &= F_s + F_g, \\ F_s &= \frac{a_1}{2}e_1^2 + \frac{a_3}{2}e_3^2 + F_l \\ F_l &= \frac{A_2}{2}e_2^2 + \frac{a_4}{4}e_2^4 + \frac{a_6}{6}e_2^6, \\ F_g &= \frac{d_2}{2}\sum_{i=1}^{3}(\nabla e_i)^2 + \frac{d_3}{4}\sum_{i=1}^{3}(\nabla^2 e_i)^2. \end{aligned} \tag{4}$$

where A_2, $a_i \quad i = 1, \ldots, 6$, d_2, and d_3 are the material-specific coefficients, and e_1, e_2, e_3 are dilatational, deviatoric, and shear components of the strains, respectively, which are defined as follows:

$$\begin{aligned} e_1 &= (\eta_{11} + \eta_{22})/\sqrt{2}, \\ e_2 &= (\eta_{11} - \eta_{22})/\sqrt{2}, \\ e_3 &= (\eta_{12} + \eta_{21})/2. \end{aligned} \tag{5}$$

Here, the Cauchy-Lagrangian strain tensor $\vec{\eta}$ is given by its components as follows:

$$\eta_{ij}(\mathbf{x}, t) = \left(\frac{\partial u_i(\mathbf{x}, t)}{\partial x_j} + \frac{\partial u_j(\mathbf{x}, t)}{\partial x_i}\right)/2, \tag{6}$$

where u_i is the displacement in the i^{th} direction in the coordinate system, $\boldsymbol{x}$ is the coordinates of a material point in the domain of interest. In this free energy functional, the deviatoric strain e_2 is chosen as the order parameter.

In the above elastic free energy function F, the Ginzburg term F_g is the term proportional to the square of the strain gradients. It produces an energy cost for deviations from spatial uniformity such as in the presence of domain walls. This term is necessary for simulation of the microstructures and phase growth ([JAC 00], [LOO 03] and references there in), but it will be neglected here as we are only interested in the properties of the material before and after the phase transformation. In this first experiment the dynamics of the transformation process, domain wall movement will not be accounted for and therefore the Ginzburg term can be omitted.

The Landau free energy function F_l can converted into a triple well, double well, or convex potential, depending on the specific temperature and the material-specific constants. To include the temperature dependency of the free energy functional, the material parameter A_2 is assumed to be linearly dependent on the material temperature $A_2 = a_2(\theta - \theta_0)$. Now, if we assume that shape

memory contributions and mechanical field contributions $\psi_1(\theta)\psi_2(\epsilon) + \psi_3(e_i)$ are represented by the above mentioned Landau free elastic energy functional, and take the thermal contribution ψ_0 the same as in the in 1D case, the final form of the Helmholtz free energy function for the square to rectangular transformations will take the following form:

$$\Psi(\theta, \epsilon) = -c_v\theta \ln\theta + \frac{a_1}{2}e_1^2 + \frac{a_3}{2}e_3^2 + F_L, \quad (7)$$

$$F_L = \frac{a_2}{2}(\theta - \theta_0)\, e_2^2 - \frac{a_4}{4}e_2^4 + \frac{a_6}{6}e_2^6. \quad (8)$$

Taken the free energy functional in the Landau form, the internal energy e can be defined as $e = \Psi - \theta\dfrac{\partial\Psi}{\partial\theta}$, and the stress-strain constitutive relationship is assumed in the standard form $\vec{\sigma} = \rho\dfrac{\partial\Psi}{\partial\vec{\eta}}$ which gives

$$\sigma_{11} = \frac{\sqrt{2}}{2}\rho(a_1e_1 + a_2(\theta - \theta_0)e_2 - a_4e_2^3 + a_6e_2^5),$$

$$\sigma_{12} = \frac{1}{2}\rho a_3e_3 = \sigma_{21},$$

$$\sigma_{22} = \frac{\sqrt{2}}{2}\rho(a_1e_1 - a_2(\theta - \theta_0)e_2 + a_4e_2^3 - a_6e_2^5).$$

By assembling the above expressions together, the governing equations for the dynamics of shape memory alloy patches with square-to-rectangular transformations can be written as:

$$\frac{\partial^2u_1}{\partial t^2} = \frac{\sqrt{2}}{2}\frac{\partial}{\partial x}(a_1e_1 + a_2(\theta - \theta_0)e_2 - a_4e_2^3 + a_6e_2^5)$$

$$+\frac{1}{2}\frac{\partial}{\partial y}(a_3e_3) + f_1,$$

$$\frac{\partial^2u_2}{\partial t^2} = \frac{1}{2}\frac{\partial}{\partial x}(a_3e_3) + \frac{\sqrt{2}}{2}\frac{\partial}{\partial x}(a_1e_1 - a_2(\theta - \theta_0)e_2$$

$$+a_4e_2^3 - a_6e_2^5) + f_2,$$

$$c_v\frac{\partial\theta}{\partial t} = k(\frac{\partial^2\theta}{\partial x^2} + \frac{\partial^2\theta}{\partial y^2}) + \frac{\sqrt{2}}{2}a_2\theta e_2\frac{\partial e_2}{\partial t} + g.$$

This model is a generalization of the well-known one-dimensional Falk model. Recall that in the one dimensional case we have to deal with two martensite variants at low temperature, one austenite at high temperature, and metastable phases in between. For such a case we have recently derived discrete analogues of conservation laws [MAT 04]. A methodology similar to that of [MAT 04] can be applied to the two dimensional case of square-to-rectangular transformations discussed here.

III. Numerical implementation

From a computational point of view, it is convenient to introduce two velocity components $v_1 = \partial u_1/\partial t$, $v_2 = \partial u_2/\partial t$, and to use them in the representation of the dilatational and deviatoric strains as follows:

$$\frac{\partial e_1}{\partial t} = (\frac{\partial v_1}{\partial x} + \frac{\partial v_2}{\partial y})/\sqrt{2},$$

$$\frac{\partial e_2}{\partial t} = (\frac{\partial v_1}{\partial x} - \frac{\partial v_2}{\partial y})/\sqrt{2}.$$

In the 2D model, we have three strain components e_1, e_2, e_3, which are dependent on the two displacements u_1, u_2. Hence, the change of variables, performed according to the above relationships, requires an additional relation, which is derived from the compatibility condition in terms of the strain components [JAC 00], [LOO 03]:

$$\frac{\partial^2e_1}{\partial x_1^2} + \frac{\partial^2e_1}{\partial x_2^2} - \sqrt{8}\frac{\partial^2e_3}{\partial x_1\partial x_2} - \frac{\partial^2e_2}{\partial x_1^2} + \frac{\partial^2e_2}{\partial x_2^2} = 0. \quad (9)$$

In the new variables, our model can be written as follows:

$$\frac{\partial e_1}{\partial t} = (\frac{\partial v_1}{\partial x} + \frac{\partial v_2}{\partial y})/\sqrt{2},\ \frac{\partial e_2}{\partial t} = (\frac{\partial v_1}{\partial x} - \frac{\partial v_2}{\partial y})/\sqrt{2},$$
$$\frac{\partial v_1}{\partial t} = \frac{\partial\sigma_{11}}{\partial x} + \frac{\partial\sigma_{12}}{\partial y} + f_1,\ \frac{\partial v_2}{\partial t} = \frac{\partial\sigma_{12}}{\partial x} + \frac{\partial\sigma_{22}}{\partial y} + f_2,$$
$$c_v\frac{\partial\theta}{\partial t} = k(\frac{\partial^2\theta}{\partial x^2} + \frac{\partial^2\theta}{\partial y^2}) + \frac{\sqrt{2}}{2}a_2\theta e_2\frac{\partial e_2}{\partial t} + g,$$
$$\sigma_{11} = \frac{\sqrt{2}}{2}(a_1e_1 + a_2(\theta - \theta_0)e_2 - a_4e_2^3 + a_6e_2^5),$$
$$\sigma_{12} = \sigma_{21} = \frac{1}{2}(a_3e_3),$$
$$\sigma_{22} = \frac{\sqrt{2}}{2}(a_1e_1 - a_2(\theta - \theta_0)e_2 + a_4e_2^3 - a_6e_2^5). \quad (10)$$

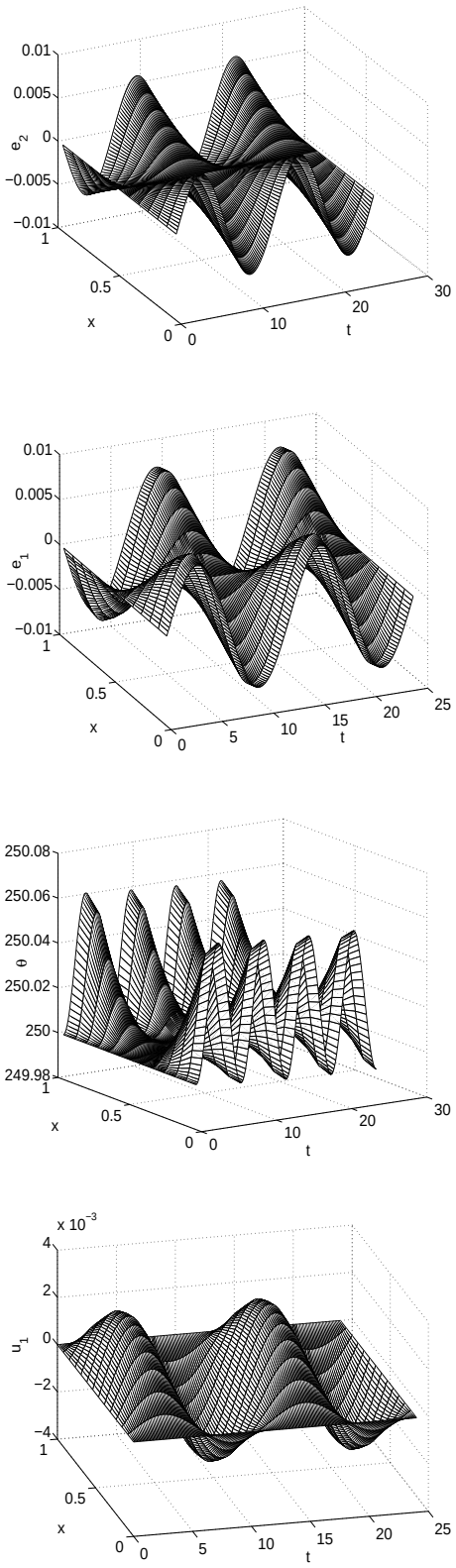

Fig. 1. Thermo-mechanical waves in a SMA patch caused by varying mechanical loadings.

Due to the presence of the stress-strain constitutive relations, viewed here as algebraic equations, the 2D model (10) is a differential-algebraic system. The idea of simulating the thermo-mechanical waves with the differential-algebraic approach stems from [MEL 00] where this approach was applied to the analysis of the dynamics of SMA rods.

We have analyzed the dynamic thermo-mechanical response of the SMA patch under varying distributed mechanical loadings, too small to induce phase transformations. The SMA patch covers an area of $1 \times 1\mathrm{cm}^2$, and we use only 14 nodes in each direction. The loading employed for this simulation is defined as $f_1 = 200\sin(\pi t/6)\mathrm{g}/(\mathrm{ms}^3\mathrm{cm})$, $f_2 = f_1$, $g = 0$, and the boundary conditions are given as $\dfrac{\partial\theta}{\partial\mathbf{n}} = 0$, $u_2 = u_1 = 0$, on all four boundaries, where $\mathbf{n}$ is the unit normal vector. The time span for this simulation is $[0, 24]$ (two periods of loading) and the time stepsize is set at 4×10^{-5}. The dilatational strain e_1, deviatoric strain e_2, temperature θ, and displacement u_1 on the central horizontal line are presented in Fig.1. The numerical results demonstrate that both the thermal and mechanical fields are driven periodically by the distributed mechanical loading due to the thermo-mechanical coupling. Under such a small loading, the SMA patch behaves in a way similar to that of a classical nonlinear thermo-elastic material. Due to symmetry in the x and y directions, distributions of temperature, displacements and strain on the central vertical line are practically identical when compared to their counterparts on the horizontal line (which are not plotted here).

The DAE system (10) is solved numerically. Velocity components v_1 and v_2 are discretized at the flux points $(x_{i+1/2}, y_{j+1/2}), x_{i+1/2} = (i + 1/2)h_x, y_{j+1/2} = (j + 1/2)h_y$ where h_x and h_y are grid size along the x and y direction, respectively, $i = 1, 2, ..., m_x$ and $j = 1, 2, ..., m_y$ with m_x and m_y being the numbers of discretisation points in the x and y directions. Variables e_1, e_2, θ, σ_{11}, σ_{12}, σ_{22} are discretized at (x_i, y_j).

The DAE system (10) can be written in the following compact form:

$$\mathbf{A}\frac{d\mathbf{U}}{dt} + \mathbf{H}\left(t, \mathbf{X}, \mathbf{U}\right) = \mathbf{0} \tag{11}$$

with matrix $A = \mathrm{diag}(a_1, a_2, ..., a_N)$ having entries "one" for differential and "zero" for algebraic equations for stress-strain relationships, and vector-function $\mathbf{H}$ defined by the right hand side parts of our system. This (stiff) system is solved with respect to the vector of unknowns $\mathbf{U}$ having $6 \times m_x \times m_y + 2 \times (m_x + 1) \times (m_y + 1)$ components by using the second order backward differentiation

formula ([HAI 96])

$$\mathbf{A}\left(\frac{3}{2}\mathbf{U}^n - 2\mathbf{U}^{n-1} + \frac{1}{2}\mathbf{U}^{n-2}\right) + \Delta t\mathbf{H}\left(t_n, \mathbf{X}, \mathbf{U}^n\right) = 0 \tag{12}$$

where n denotes the current time layer.
We note that in order to deal with strong nonlinearities in the order parameter, a smoothing procedure similar to that discussed in [NIE 91], [MAT 04] has been employed during the integration process here. In particular, we have used the following expansions:

$$y^3 = \frac{1}{4}\sum_{i=0}^{3} y_n^i y_{n-1}^{3-i}; \quad y^5 = \frac{1}{6}\sum_{i=0}^{5} y_n^i y_{n-1}^{6-i}, \tag{13}$$

where y_n is the unknown variable on the current time layer n while y_{n-1} is the unknown variable on the previous time layer $n-1$ (for 2D problem, $y = e_2$, while for 1D case $y = \epsilon = \partial u/\partial x$). In its essence, nonlinear terms are averaged here in the Steklov sense, so that for nonlinear function $f(y)$ (in particular, y^3 and y^5), averaged in the interval $[\epsilon_{n-1}, \epsilon_n]$, we have

$$g(y_{n-1}, y_n) = \frac{1}{y_n - y_{n-1}}\int_{y_{n-1}}^{y_n} f(\eta)d\eta, \tag{14}$$

where $y_{n-1} = y(t_{n-1})$, $y_n = y(t_n)$.

IV. Numerical experiments

The mathematical model discussed in the previous sections has been analysed on a series of numerical experiments, some of which are reported below. First, we performed simulations with $Au_{23}Cu_{30}Zn_{47}$. For this specific material, all physical parameters for the 1D Falk model are available in the literature [FAL 80], [MEL 01], [NIE 91]. For the 2D model (10), there are no experimental values readily available. Here, we take all the parameters in the Landau free energy function in the 2D model the same as those in the 1D case [MAT 04], [WAN 04]. This gives us $a_2 = k_2, a_4 = k_2, a_6 = k_3$. Then, we take the values $a_1 = 2a_2$ and $a_3 = a_2$, as suggested in [JAC 00], [CUR 01]. All the thermal parameters are taken the same as in the 1D case. The initial and boundary conditions for these simulations were taken as:

$$\theta^0 = 250^o\mathrm{K}, \epsilon^0 = v^0 = \sigma^0 = 0 \tag{15}$$

$$\frac{\partial\theta}{\partial n} = 0, \quad u_2 = u_1 = 0, \quad \text{on the four boundaries.} \tag{16}$$

Because the displacement components are already replaced by the strains in (10), the above boundary conditions are enforced in terms of velocity components. We used the following periodic mechanical loading:

$$f_1 = f_2 = 6000\begin{cases} \sin(\pi t/3), & 0 \le t \le 4, \\ 0, & 4 \le t \le 6, \\ \sin(\pi(t-2))/3), & 6 \le t \le 10, \\ 0, & 10 \le t \le 12. \end{cases} \tag{17}$$

Similarly to the analysis of 1D phase transformations, one can easily calculate the deviatoric strains that correspond to austenite and martensite variants in the SMA patch. In minimizing the Landau free energy functional, the condition $\partial F_l/\partial e_2 = 0$ yields:

$$e_2 = 0; \quad e_2^2 = \frac{a_4 \pm \sqrt{a_4^2 - 4a_2 d\theta a_6}}{2a_6},$$

where $d\theta$ is the difference between the current material temperature and the transformation temperature. Obviously, $e_2 = 0$ corresponds to the austenite. Let us denote $(a_4 + \sqrt{a_4^2 - 4a_2 d\theta a_6})/2a_6$ by e_m. Then $e_{2+} = +\sqrt{e_m}$ or $e_{2-} = -\sqrt{e_m}$ are the strains that correspond to the two martensite variants, martensite plus and martensite minus. It can be estimated, given the initial temperature, that $d\theta = 42^o$ which gives us $e_{2+} = 0.12$ and $e_{2-} = -0.12$.
In the experiment reported here, we applied the mechanical loading only in the x direction, while there was no loading in the y direction. In this case, there is no symmetry along the diagonal line , but there is symmetry along the middle vertical line $x = 0.5$. Naturally, one would expect that the SMA patch will be divided by a symmetry line into martensite plus and martensite minus. The numerical results for this experiment are shown as the distributions of e_2, u_1, e_1, and θ in Fig. 2. As expected, the martensitic transformations are induced by the mechanical loading periodically, and the SMA patch is divided by the interface into martensite plus and martensite minus each time after the transformation is completed. Furthermore, the combination of the martensite variants is also changing periodically.
The developed methodology was applied also to modelling AlCuZn patches. Although the example that follows is somewhat artificial, it allows us to verify whether there is any substantial difference between square to rectangular transformation with different material specific parameters. Physical parameters for this material for the 1D case are available from [BUB 96]. We artificially enlarged the specific heat by the factor of 10 in order to make the temperature of this material barely sensitive to the work done on it (otherwise stability problems arise). As we explained above, we obtained estimates of the parameters in the 2D model. We performed simulations on a the $1 \times 0.5\mathrm{cm}^2$ AlCuZn rectangular patch. The initial and boundary conditions were taken as follows:

$$\theta^0 = 360^o\mathrm{K}, \epsilon^0 = v^0 = \sigma^0 = 0 \tag{18}$$

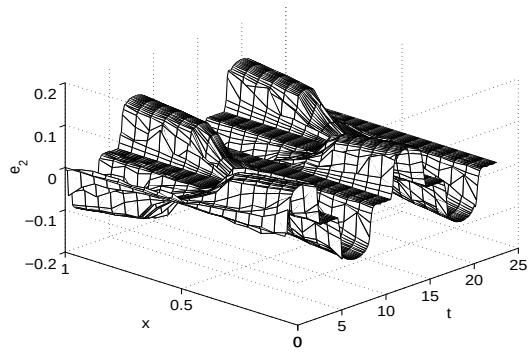

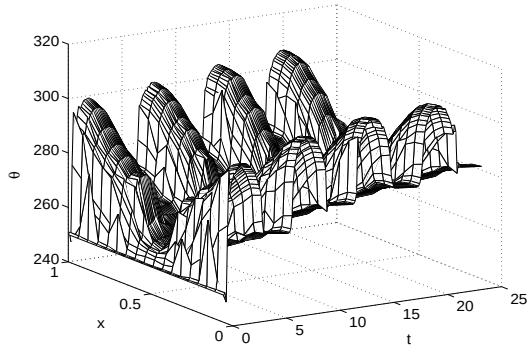

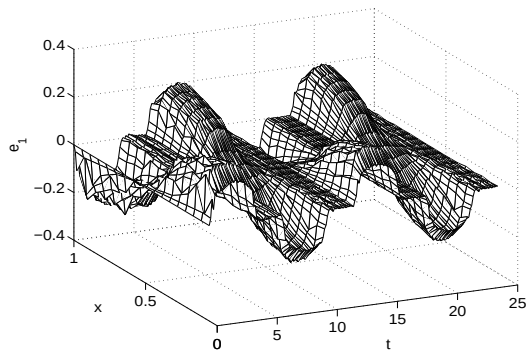

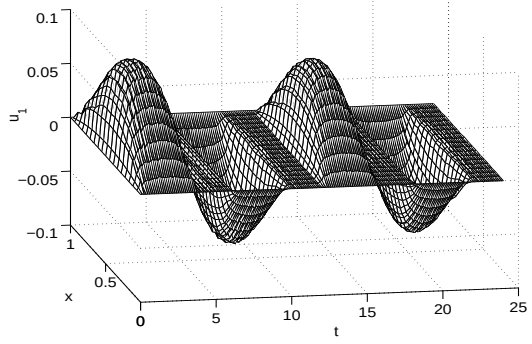

Fig. 2. Martensitic transformations in SMA patches caused by mechanical loadings only in the x direction.

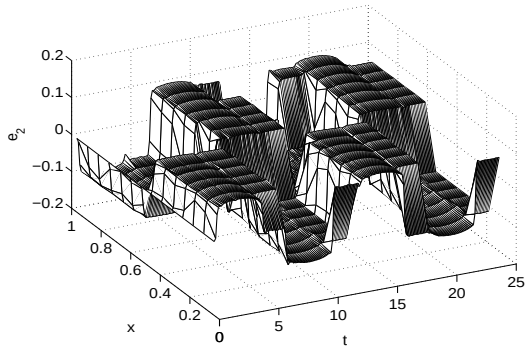

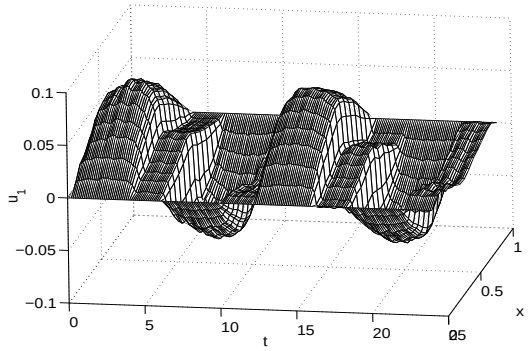

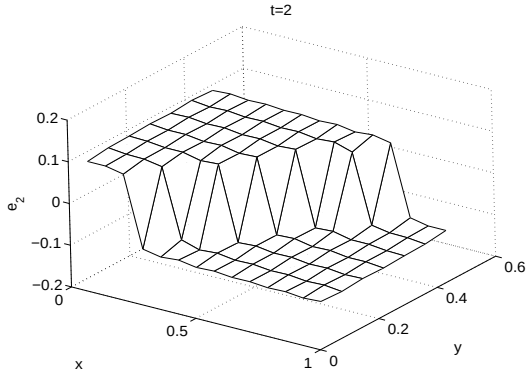

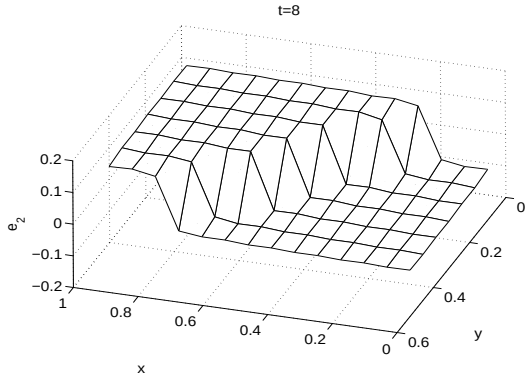

Fig. 3. Martensitic transformations in a rectangular $CuZnAl$ patch caused by mechanical loadings in the x and y direction.

$$\frac{\partial \theta}{\partial n} = 0, \quad u_2 = u_1 = 0, \quad \text{on the four boundaries.} \quad (19)$$

We employed the following loading:

$$f_1 = f_2 = 1200 \begin{cases} \sin(\pi t/3), & 0 \le t \le 4, \\ 0, & 4 \le t \le 6, \\ \sin(\pi(t-2))/3), & 6 \le t \le 10, \\ 0, & 10 \le t \le 12. \end{cases} \quad (20)$$

Due to the imposed boundary conditions, we expect that after the transformation, the martensite combination should be similar to its counterpart in the experiment where the loading is applied in both x and y directions, but scaled along the y direction. The numerical results presented in Fig. 3 confirm that.

REFERENCES

[LAN 04] LANGER, R. and TIRRELL, D.A., Designing materials for biology and medicine, 428 (6982), p. 487–492, Nature, 2004.

[KUJ 04] KUJALA, S. et al, Biocompatibility and strength properties of nitinol shape memory alloy suture in rabbit tendon, vol. 25(2), p. 353–358, Biomaterials, 2004.

[BIR 97] BIRMAN, V., Review of mechanics of shape memory alloys structures, vol. 50, p. 629-645, Appl.Mech.Rev., 1997.

[MEL 01] MELNIK, R., ROBERTS, A., THOMAS, K., Coupled thermomechanical dynamics of phase transitions in shape memory alloys and related hysteresis phenomena, vol. 28(6), p. 637-651, Mechanics Research Communications, 2001.

[MEL 02] MELNIK, R., ROBERTS, A., THOMAS, K., Phase transitions in shape memory alloys with hyperbolic heat conduction and differential algebraic models, 29(1), p. 16–26, Computational Mechanics, 2002.

[BUB 96] BUBNER, N., Landau-Ginzburg model for a deformation-driven experiment on shape memory alloys, vol. 8, p. 293-308, Continuum Mech. Thermodyn., 1996.

[FAL 90] FALK, F., KONOPKA, P., Three-dimensional Landau theory describing the martensitic phase transformation of shape memory alloys, vol. 2, p. 61-77, J.Phys.:Condens.Matter, 1990.

[PAW 00] PAWLOW, I., Three dimensional model of thermomechanical evolution of shape memory materials, vol. 29, p. 341-365, Control and Cybernetics, 2000.

[ERI 86] ERICKSEN,J.L., Consitutive theory for some constrained elastic crystals, vol. 22, p. 951-964, J.Solids and Structures, 1986.

[ICH 00] ICHITSUBO, T., TANAKA, K., KOIVA, M.,YAMAZAKI, Y., Kinetics of cubic to tetragonal transformation under external fi eld by the time-dependent Ginzburg-Landau approach, vol. 62(9), p. 5435-5441, Phys. Rev. B, 2000.

[JAC 00] JACOBS, A., Landau theory of structures in tetragonal-orthorhombic ferro-elastics, vol. 61(10), p. 6587-6595, Phys. Rev. B, 2000.

[MAT 04] MATUS, P., MELNIK, R.V.N., WANG, L., RYBAK, I., Applications of fully conservative schemes in nonlinear thermoelasticity: modelling shape memory materials, vol. 65(4-5), p. 489–510, Mathematics and Computers in Simulation, 2004.

[MEL 00] MELNIK, R., ROBERTS, A., THOMAS, K., Computing dynamics of Copper-based SMA via center manifold reduction models, vol. 18, p. 255-268, Computational Material Science, 2000.

[LOO 03] LOOKMAN, T. et al, Ferro-elastic dynamics and strain compatibility, vol. 67, p. 024114, Phys. Rev. B, 2003.

[SAX 98] SAXENA, A., BiSHOP, A., SHENOY, S., LOOKMAN, T., Computer simulation of martensitic textures, vol. 10, p. 16-21, Computational Materials Science, 1998.

[KAR 95] KARTHA, S., Disorder-driven pretransitional tweed pattern in martensitic transformations, vol. 52(2), p. 803-823, Phys. Rev. B, 1995.

[BAL 88] BALL, R., JAMES, M., Fine phase mixtures as minimizers of energy, vol. 100, p. 13-52, Archive. Rat. Mach. Anal., 1988.

[FAL 80] FALK, F., Model free energy, mechanics, and thermomechanics of shape memory alloys, vol. 28, p. 1773-1780, Acta Metallurgica, 1980.

[HAI 96] HAIRER,E., NORSETT,S.P., and WANNER,G., Solving ordinary differential equations II-stiff and differential algebraic problems, Springer-Verlag, Berlin, 1996.

[NIE 91] NIEZGODKA, M., SPREKELS, J.: Convergent numerical approximations of the thermomechanical phase transitions in shape memory alloys, vol. 58, p. 759-778, Numerische Mathematik, 1991.

[WAN 04] WANG, L. and MELNIK, R.V.N., Thermomechanical waves in SMA patches under small mechanical loadings, vol. 3039, p. 645-652, in Lecture Notes in Computer Science, Eds. M.Bubak, G.Dick, v.Albada, P.M.A.Sloot, and J.Dongarra, Springer,Berlin, 2004.

[CUR 01] CURNOE,S.H., JACOBS, A.E., Time evolution of tetragonal-orthorhombic ferroelastics, vol. 64, p. 064101, Physical Rev. B, 2001.

Honorary Chair:
Prof. Robert Vichnevetsky, Rutgers University - USA

General Chair:
Prof. Pierre Borne, Ecole Centrale de Lille - France

International Program Committee Chair:
Prof. Mohamed Benrejeb, ENIT - Tunisia
Prof. Spyros Tzafestas, NTUA - Greece
Prof. Serge Petiton, LIFL/INRIA - France

ECOLE CENTRALE DE LILLE
Cité Scientifique - BP 48
59651 Villeneuve d'Ascq Cedex - France
Phone: (33/0)3 20 33 53 53
Fax: (33/0)3 20 33 54 99
http://imacs2005.ec-lille.fr

ISBN: 2-915913-02-1
EAN: 9782915913026

Edited by:
Pierre Borne
Mohamed Benrejeb
Nathalie Dangoumau
Lionel Lorimier

17th IMACS World Congress

Scientific Computation, Applied Mathematics and Simulation

http://imacs2005.ec-lille.fr

Paris, France / July 11 - 15, 2005

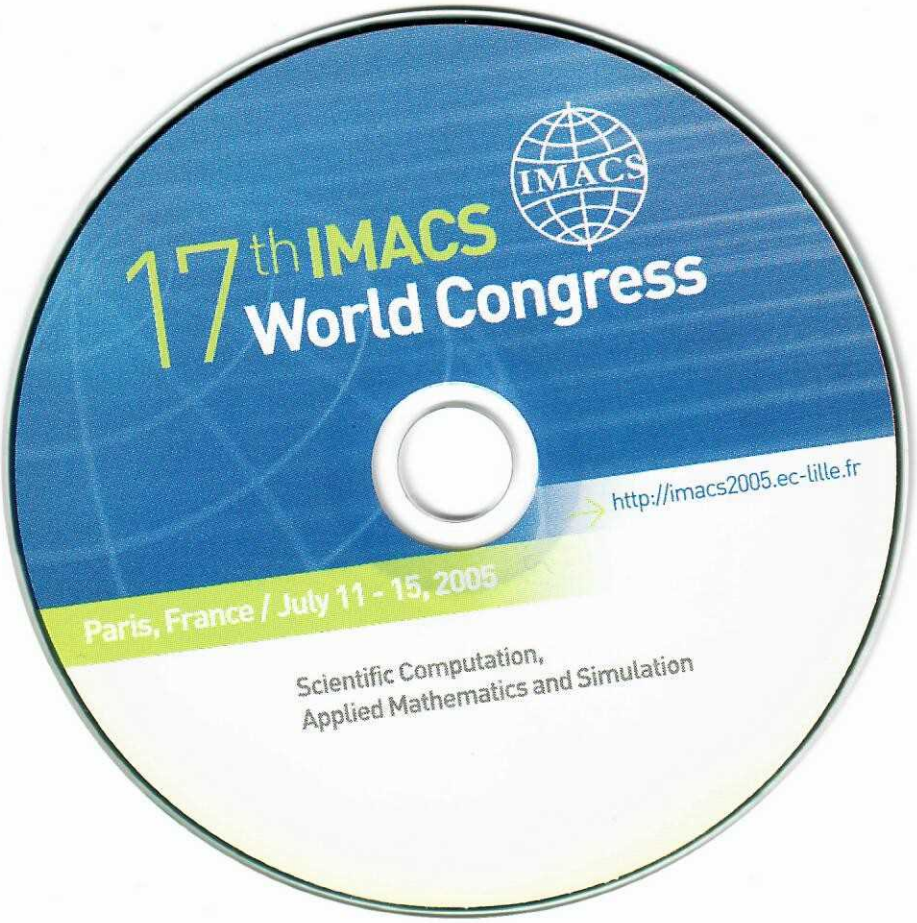
IMACS
17th IMACS
World Congress
http://imacs2005.ec-lille.fr
Paris, France / July 11 - 15, 2005
Scientific Computation,
Applied Mathematics and Simulation